

# POWER SYSTEM STABILITY ASSESSMENT FOR KARNALI PROVINCE OF NEPAL

Navaraj Shrestha<sup>1\*</sup>, Shreeshuva Maharjan<sup>1</sup>, Aayush Bista<sup>1</sup>, Samundra Gurung<sup>1</sup>, Sadam Bala<sup>2</sup>, Diwakar Bista<sup>1</sup>

<sup>1</sup> Department of Electrical and Electronics Engineering, Kathmandu University

<sup>2</sup> Nepal Electricity Authority, Government of Nepal

---

## Abstract

Karnali province in Nepal faces significant challenges in ensuring a stable and reliable power supply due to its weak transmission network, high system losses, and limited local generation capacity. Therefore, there is a high need for the assessment of the performance and power system stability of the current Karnali grid to mitigate any potential issues that can occur due to the addition of load. This paper conducts a comprehensive assessment of the existing Karnali province power grid to identify major performance bottlenecks and stability issues, covering voltage, angle (transient and small signal), and frequency stability, which were performed under four operational scenarios: base case, increased load, reduced load, and N-1 contingency. Results indicate the significant voltage drop and low voltage stability margins in multiple substations, especially in Khalanga, Manma, and Kudu substations. Modal analysis revealed critical buses and branches, which are prone to voltage instability. This study shows that the voltage stability margin and reactive power margin of the Karnali province power grid are low and decrease with increasing load demand. Small signal stability analysis shows a poorly damped local mode with a damping ratio as low as 5.61% in the increased load scenario, while transient stability shows a narrow critical clearing time, approximately 0.34 seconds in the decreased load condition. Frequency stability was within operational limits, showing robustness under disturbances.

**Keywords:** Voltage stability, Frequency stability, Angle stability, Modal analysis, Eigen value

---

## 1. Introduction

The power system of Nepal has witnessed significant growth in the past few years, driven largely by the development of hydropower resources and the expansion of national transmission infrastructure. The Nepal Electricity Authority (NEA), Nepal's utility grid, connects various provinces via a network with a wide voltage range. Despite this progress, geographical barriers, isolated load centers, and long transmission corridors all have an impact on the grid's robustness. In particular, provinces like Karnali, characterized by mountainous terrain and limited industrial load, experience difficulties in ensuring a stable and reliable power supply. One of the major problems faced in Karnali is the lack of dedicated high-capacity transmission lines and

the 33 kV and 11 kV distribution systems. With several hydropower projects planned and under-construction of the Kohalpur-Surkhet-Dailekh 132 kV transmission line, the stability assessment of the local power system becomes vital to support future grid integration and development. Power system stability has been recognized as an important factor for secure system operation. Many major blackouts caused by power system instability have illustrated the importance of this phenomenon (Wu et al., 2017). The ability of an electric power system to regain a state of operating equilibrium after being subjected to a physical disturbance, for a given initial operating condition, is said to be power system stability (Hatziaargyriou et al., 2020). Traditionally, the power system is categorized into three main groups: Rotor angle stability, Voltage stability, and Frequency stability (Kundur et al., 2017). Voltage stability refers to the ability of a power system to maintain steady voltage at all buses in the system after being subjected to a disturbance from a given initial operating condition.

---

\*Corresponding author: Navaraj Shrestha  
Department of Electrical and Electronics Engineering, KU  
Email: navaraj0123@student.ku.edu.np  
<https://doi.org/10.3126/jsce.v12i2.91410>

There are several methods to assess the voltage strength of a system, such as PV curve, QV curve, and modal analysis (Morison et al., 1993). The ability of a power system to maintain steady frequency following a severe system disturbance resulting in a significant imbalance between generation and load is said to be frequency stability. The system frequency behavior following a disturbance, such as a generator outage, can be assessed using indices like the Rate of Change of Frequency (RoCoF) and the center of inertia frequency ( $f_{COI}$ ) (Sun et al., 2021). The angle stability is further subdivided into transient stability and small signal stability (SSS). Transient stability refers to the ability of the power system to maintain synchronism in the presence of any severe transient disturbance. The transient stability can be studied by using critical clearing time ( $T_{cl}$ ) and the Transient stability index (TSI) (Shi et al., 2009). The ability of the system to maintain synchronism when subjected to small disturbances, such as minor load variations or small changes in generation, is said to be small signal stability (Hatziaargyriou et al., 2020). SSS is widely analyzed by using the modal/eigenvalue analysis (Gurung et al., 2020).

Several studies have been conducted globally and within Nepal to assess power system stability under various scenarios. The authors of (Islam et al., 2017) use EDSA Paladin Design Base Software to examine the transient response and voltage stability of the northern part of Bangladesh's power grid. In the paper (Cho et al., 2021), the probabilistic transient stability assessment method has been employed to evaluate the effects of high renewable energy penetration on Korea's power system. The authors of (Eftekharijad et al., 2013) investigate the effects of high penetration of photovoltaic (PV) systems on the small signal stability of power systems, emphasizing the challenges posed by reduced system inertia and altered power flow patterns. In the paper (O'Sullivan et al., 2014), the authors have studied how high levels of non-synchronous generation (mainly wind and HVDC) affect frequency stability in Ireland's isolated power system. The authors of (Shrestha et al., 2024) have identified the critical issues in angle, voltage, and frequency stability of the power system of Nepal.

In this study, the Karnali province power grid is modeled and analyzed using DIgSILENT PowerFactory in order to assess its present performance and pinpoint major issues such as voltage stability, transient stability, small signal stability, and frequency stability.

The remainder of this paper is organized as follows: Section 2 presents the system description of Karnali province power grid, and Section 3 highlights the methodology used for power system stability assessment. Section 4 discusses the simulation results and evaluates system performance under various disturbance scenarios. Section 5 concludes

the paper, summarizing key findings.

## 2. System Description

Two hydropower generation, i.e., Naumule P/S, and Rukumgad P/S is connected to the power grid of Karnali province. Kohalpur grid is designated as the slack bus in this study. The modeled system consists of 22 buses, 1 generator, and 10 loads. The total generation capacity and load for the modeled system are 3.75 MW and 14.49 MW, respectively. Voltage levels of 11 kV and 33 kV have been considered. The model includes eleven 33 kV lines with a total length of 401 km. Only the existing Karnali province power grid is considered in this study. The Musikot S/S, Tharmare S/S, and Rukumgad P/S are not included because they are isolated from the grid. The model of the Karnali power grid is shown in Figure 1.

## 3. Methodology

Karnali province's power system stability was evaluated using a systematic, multi-phase methodology designed to find potential issues. The three main phases of this method are system modeling and component selection, stability performance analysis, and result interpretation, which is as shown in Figure 2. DIgSILENT PowerFactory was used throughout the process to accurately model and simulate the Karnali grid.

In the first stage, a detailed electrical model of the Karnali province power system was developed. The generator dynamic models followed IEEE3 governor standards and IEEE1S excitation system standards. Loads were modeled using a combination of 70% static and 30% dynamic components, in order to demonstrate the real-world case, with the static portion represented by the ZIP (constant impedance, current, and power) model.

The second stage focused on performance analysis through various simulation techniques. Load flow analysis was performed initially to assess voltage profiles, power flows, and the loading of lines. For stability assessment, time-domain simulations were conducted to evaluate transient and frequency stability. Additionally, modal analysis techniques were employed to assess small signal and voltage stability.

The final stage involved the interpretation of results from the simulations and analyses.

## 4. Results and Discussion

The results obtained through the application of above mentioned methodology are presented here. The performance parameter related to voltage, frequency, and angle stability of power system have been calculated. The results are obtained and analyzed under different scenarios as listed in Table 1. For the scenario 2 and 3, increased load

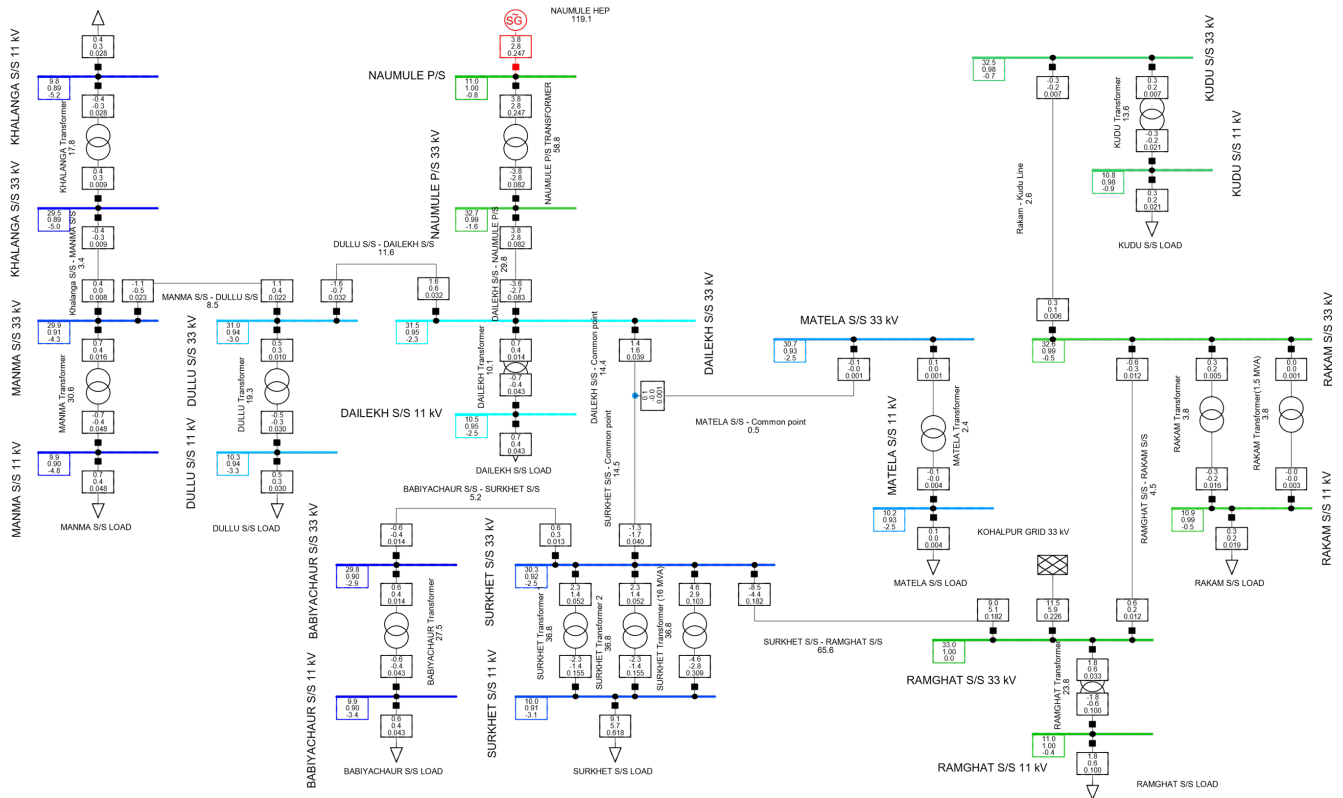


Figure 1. Model of Karnali province power grid.

Table 1. Description of the scenarios considered.

Scenario	Name	Description
1	Base Case	-
2	Increased Load Condition	Load is equal to Maximum Load
3	Decreased Load Condition	Load is equal to 50% of Maximum Load
4	N-1 Contingency Condition	Disconnection of SURKHET Transformer (16 MVA)

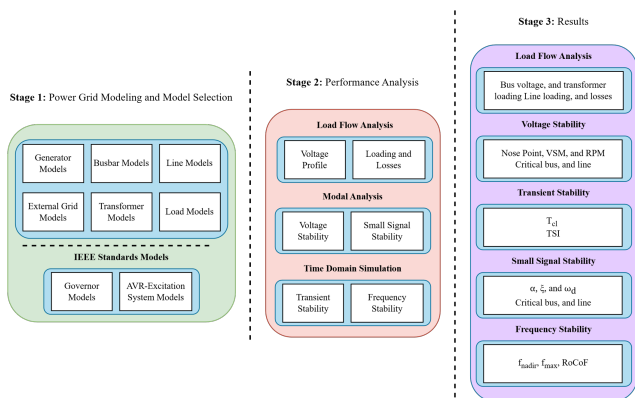


Figure 2. Methodology for performance analysis of Karnali province power grid.

condition is considered as maximum load of the system and decreased load condition is considered as 50% of maximum load respectively. Additionally, for the N-1 contingency

condition, the study considers the highest rated transformer, specifically the 16 MVA Surkhet transformer. Since all lines are radial and single circuit, if a line made outage, the substation connected by that line will be out of operation.

#### 4.1. Load Flow Results

Figure 3 shows the bus voltage profile of different substations under different scenarios. Khalanga, Babiychaur, Manma, Surkhet, Matela, and Dullu substations operate below the acceptable lower voltage limit of 0.95 p.u. under all scenarios considered.

#### 4.2. Voltage Stability Results

In this paper, voltage stability is studied by PV curve, QV curve, and the modal analysis method.

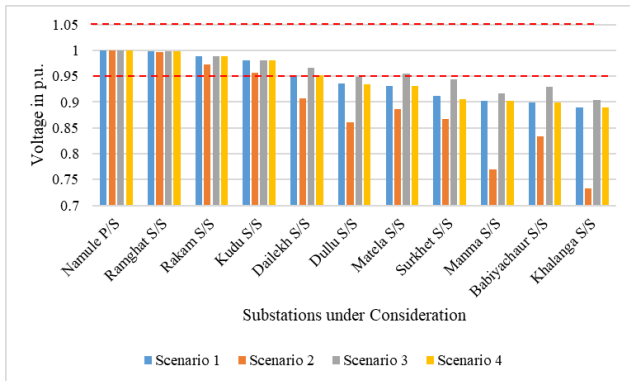


Figure 3. Voltage profile of substations under different scenarios.

#### 4.2.1 PV Curve Results

The voltage stability margin (VSM) of substations under different scenarios is presented in Table 2. Khalanga S/S shows a low VSM of 0.73 MW under scenario 2, while Ramghat S/S has the highest VSM of 72.94 MW under scenario 3. Substations like Ramghat, Surkhet, Dailekh, and Rakam have high voltage stability margins, whereas Khalanga, Manma, and Kudu have much lower reserves.

Table 2. VSM of substations under different scenarios.

Substations Name	Voltage Stability Margin, VSM (MW)			
	Scenario 1	Scenario 2	Scenario 3	Scenario 4
Khalanga S/S	1.5953	0.7278	1.6632	1.5927
Manma S/S	2.7041	1.2509	2.8256	2.6992
Kudu S/S	4.5555	4.1307	4.5555	4.5555
Babiyachaur S/S	4.8035	3.629	5.2291	4.791
Dullu S/S	6.4472	3.6734	6.7891	6.4369
Matela S/S	6.7848	5.5628	7.2589	6.7631
Rakam S/S	9.4621	8.8519	9.4621	9.4621
Dailekh S/S	10.5753	6.3761	11.7381	10.5376
Surkhet S/S	16.9185	11.1421	20.3449	15.4973
Ramghat S/S	72.4258	71.6514	72.9422	72.4258

#### 4.2.2 QV Curve Results

Khalanga S/S, and Manma S/S have significantly lower reactive power margin (RPM) of 1.0485 MVar, and 1.8098 MVar respectively, while Ramghat S/S and Surkhet S/S have strong voltage stability reserve of 66.24 MVar and 28.69 MVar respectively under different scenarios, as shown in Table 3.

#### 4.2.3 Modal Sensitivity Results

The Modal Sensitivity Analysis results highlight the critical buses and lines by evaluating eigenvalues and participation factors. The results obtained by application of modal voltage stability analysis in the modeled system are shown in Table 4. This study examines five critical

Table 3. RPM of substation under different scenarios.

Substations Name	Reactive Power Margin, RPM (MVar)			
	Scenario 1	Scenario 2	Scenario 3	Scenario 4
Khalanga S/S	2.0526	1.0485	2.1314	2.0497
Manma S/S	3.4617	1.8098	3.5969	3.4565
Kudu S/S	5.3889	4.9869	5.3889	5.3889
Babiyachaur S/S	5.6905	4.5122	6.1523	5.6736
Matela S/S	7.8026	6.7897	8.2596	7.7857
Dullu S/S	7.8801	5.2785	8.1626	7.8709
Rakam S/S	11.3988	10.8232	11.3988	11.3988
Dailekh S/S	19.3416	13.2050	20.1535	19.3096
Surkhet S/S	24.8258	17.6827	28.6901	21.7071
Ramghat S/S	66.0620	65.7955	66.2373	66.0620

modes for further analysis. The smallest eigenvalue of 3.6106 MVar/p.u. indicates the weakest mode, implying that this mode is most vulnerable to voltage instability. Subsequently, participation factor analysis has been done for modes 1-5. The results for the critical bus and line are presented in Table 5 and Table 6 respectively. In Mode 1, Khalanga S/S 11 kV exhibits the highest participation factor indicating a critical bus for voltage stability concerns. Similarly, Kudu S/S 11 kV has most contribution to mode 2, Babiyachaur S/S 11 kV has high contribution to mode 3-4, and Matela S/S 11 kV make a significant contribution to mode 5. In Table 6, a common point represents junction on the 33 kV line, where the feeder to Matela Substation taps-off from the main Surkhet–Dailekh line, located 22 km from Dailekh Substation, 14 km from Surkhet Substation, and 24 km from Matela Substation.

Table 4. Five smallest eigenvalues for scenario 1.

Mode no.	Eigenvalues $\lambda$ , (MVar/p.u.)
1	3.6106
2	11.0852
3	13.7627
4	21.2856
5	27.3897

#### 4.3. Small Signal Stability Results

The system exhibits one critical mode i.e., local nature. The local mode is participated in by the generators of Naumule HEP. Scenario 2 records the lowest damping ratio at 5.61%, indicating proximity to small signal instability. In comparison, the overall Nepal power system also exhibits a local mode, with the lowest damping ratio of approximately 2.8% (Shrestha et al., 2024). Table 7 shows the results obtained by performing eigenvalue analysis for the modeled grid.

Table 5. Buses with the highest participation for smallest eigenvalues for scenario 1.

Mode no.	Bus	Participation factor
1	Khalanga S/S 11 kV	0.2879
	Khalanga S/S 33 kV	0.2625
	Manma S/S 11 kV	0.1501
	Manma S/S 33 kV	0.1360
	Dullu S/S 11 kV	0.0303
2	Kudu S/S 11 kV	0.4079
	Kudu S/S 33 kV	0.3187
	Rakam S/S 11 kV	0.1418
	Rakam S/S 33 kV	0.1317
	Babiyachaur S/S 11 kV	0.0000
3	Babiyachaur S/S 11 kV	0.2877
	Babiyachaur S/S 33 kV	0.2030
	Matela S/S 11 kV	0.1205
	Matela S/S 33 kV	0.0874
	Khalanga S/S 11 kV	0.0496
4	Babiyachaur S/S 11 kV	0.1826
	Khalanga S/S 11 kV	0.1654
	Dullu S/S 11 kV	0.1087
	Babiyachaur S/S 33 kV	0.1045
	Khalanga S/S 33 kV	0.0946
5	Matela S/S 11 kV	0.3662
	Matela S/S 33 kV	0.1822
	Babiyachaur S/S 11 kV	0.1169
	Manma S/S 11 kV	0.0897
	Babiyachaur S/S 33 kV	0.0555

Table 6. Lines with the highest participation for smallest eigenvalues for scenario 1.

Mode no.	Branch/Line	Participation factor
1	Dailekh S/S - Common point	0.2960
2	Surkhet S/S - Common point	0.1855
3	Manma S/S - Dullu S/S	0.0180
4	Dullu S/S - Dailekh S/S	0.0129
5	Babiyachaur S/S - Surkhet S/S	0.0003

#### 4.4. Transient Stability Results

Transient stability is examined by applying a self-clearing fault near the largest generator, i.e., Naumule HEP, at 1 second. Table 8 summarizes the system's Critical Clearing Time ( $T_{cl}$ ) and Transient Stability Index (TSI) under all scenarios. The findings show that the system loses transient stability at 0.36 seconds in the base case. Among all scenarios, scenario 3 records both the lowest  $T_{cl}$  at 0.34 seconds and the lowest TSI with 68.22%, indicating a reduced transient stability margin under decreased load conditions. In comparison, the overall Nepal power system is reported to lose transient stability at a higher clearing time of approximately 0.55 seconds under normal loading conditions (Shrestha et al., 2024), indicating relatively stronger transient stability at the national grid level. Figure

4, Figure 5, Figure 6 and Figure 7 illustrate the behavior of generator rotor angles under disturbances for all of the 4 scenarios.

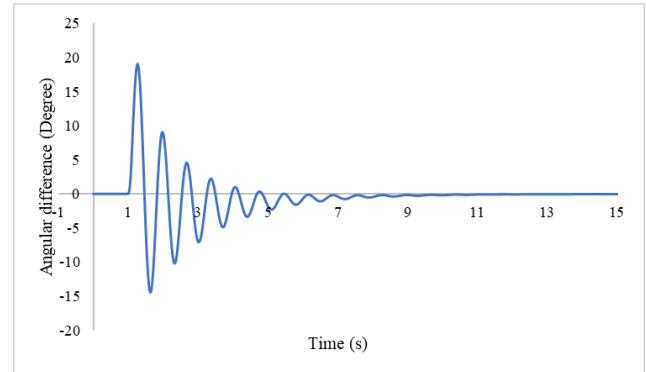


Figure 4. Time response of the relative rotor angle of the generator for scenario 1 under transient stable conditions.

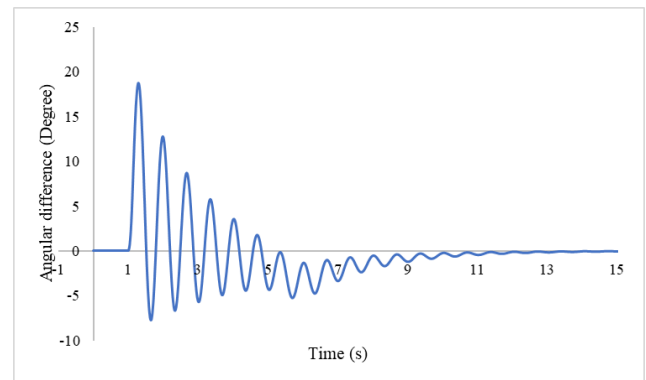


Figure 5. Time response of the relative rotor angle of the generator for scenario 2 under transient stable conditions.

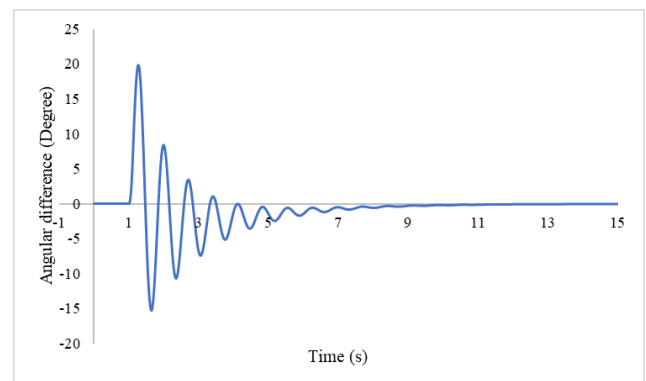


Figure 6. Time response of the relative rotor angle of the generator for scenario 3 under transient stable conditions.

Table 7. SSS results under different scenarios.

Scenario	Mode No.	Real part, $\alpha$ (1/s)	Imaginary part (rad/s)	Damping Freq, $\omega_d$ (Hz)	Damping Ratio, $\zeta$ (%)	Participating States	Type
1	Mode 00001	-1.0937	14.8183	2.3584	7.3609	Naumule HEP	Local
2	Mode 00002	-0.5243	9.3236	1.4839	5.6147	Naumule HEP	Local
3	Mode 00002	-0.7561	8.7695	1.3957	8.5905	Naumule HEP	Local
4	Mode 00002	-0.6909	8.9398	1.4228	7.7053	Naumule HEP	Local

Table 8. Transient stability indices for different scenarios.

Scenario	$T_{cl}$ (s)	TSI (%)
1	0.36	73.06
2	0.40	83.38
3	0.34	68.22
4	0.36	73.16

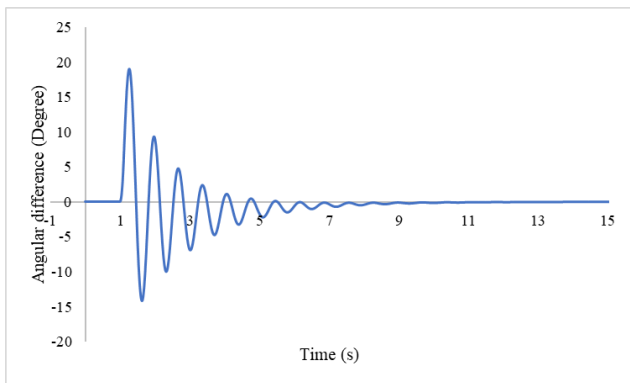


Figure 7. Time response of the relative rotor angle of the generator for scenario 4 under transient stable conditions.

#### 4.5. Frequency Stability Results

The under-frequency event is analyzed by removing the generator of Naumule HEP at 1 second. Similarly, the over-frequency event was studied by removing the largest load, i.e., Surkhet S/S load at 1 second. Under-frequency events and over-frequency events were created and analyzed separately. Figure 8, Figure 9, Figure 10 and Figure 11 depict the system's Center of Inertia (COI) frequency during the outages for scenarios 1 to 4. The plots show that the frequency remains well within the permissible  $\pm 2.5\%$  range, set by Nepal's power system operator, indicating a strong frequency stability margin. Table 9 further details that the system's minimum and maximum frequencies are 49.99 Hz and 50.05 Hz, respectively. Additionally, the maximum values of RoCoF+ (during generator outage) and RoCoF- (during load outage) are 0.0541 Hz/s and 0.0369 Hz/s, respectively. In comparison, the overall Nepal power system records  $f_{nadir}$  and  $f_{max}$  values of 49.3792 Hz and 50.1617 Hz, respectively, under the largest generator and load outages (Shrestha et al., 2024), which also remain within the prescribed operational limits.

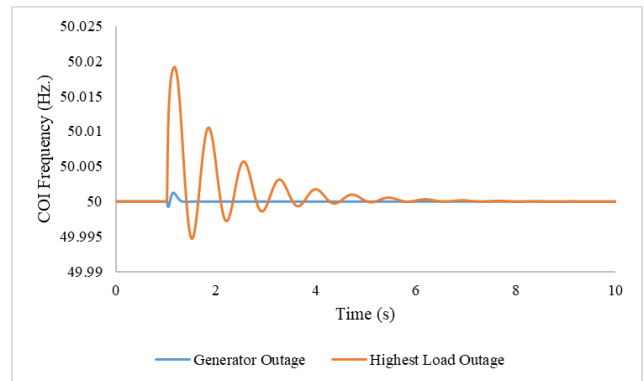


Figure 8. System COI frequency under outages for scenario 1.

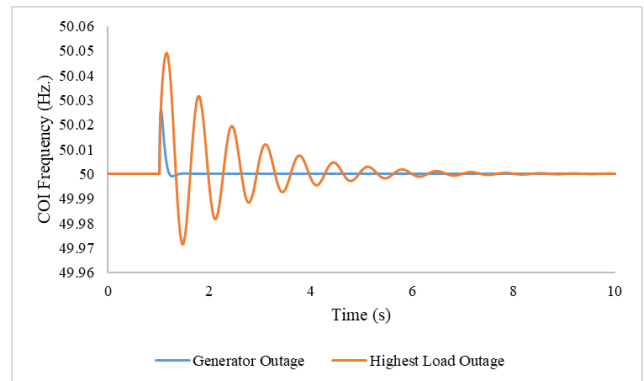


Figure 9. System COI frequency under outages for scenario 2.

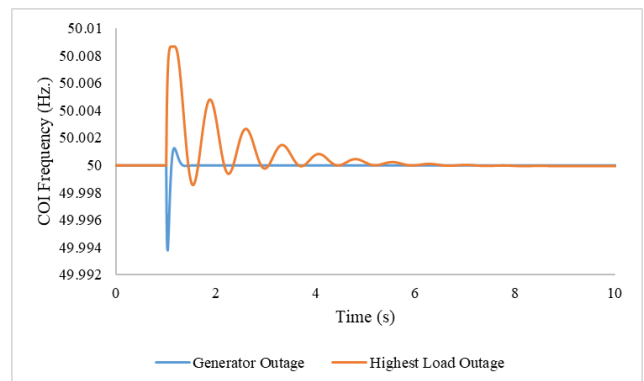


Figure 10. System COI frequency under outages for scenario 3.

Based on the identified technical issues, several mitigation strategies can be adopted to enhance the performance and reliability of the Karnali power grid

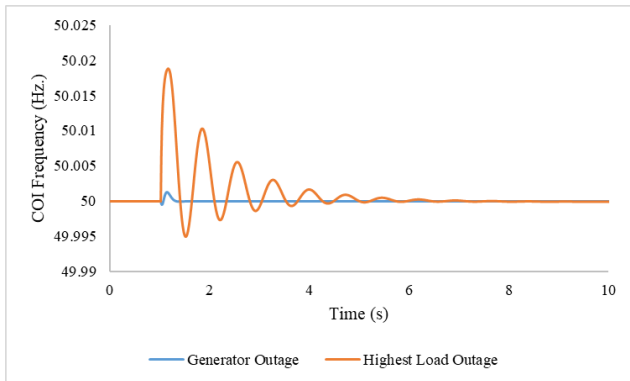


Figure 11. System COI frequency under outages for scenario 4.

Table 9. Frequency stability indices for different scenarios.

Scenario	$f_{nadir}$ (Hz)	RoCoF- (Hz/s)	$f_{max}$ (Hz)	RoCoF+ (Hz/s)
1	49.99	0.0369	50.02	0.1276
2	49.99	0.0201	50.05	0.3499
3	49.99	0.2077	50.01	0.0541
4	49.99	0.0234	50.02	0.1255

in compliance with NEA grid standards. Voltage violations observed at remote substations, where bus voltages fall below the permissible range of 0.95 - 1.05 pu under high loading and N-1 contingencies, can be mitigated through optimal placement of shunt capacitors and FACTS devices, along with effective On-Load Tap Changer (OLTC) operation. Reactive power compensation at voltage-collapse-prone substations is recommended to improve voltage stability margins and reduce system losses. Thermal overloading of the transmission lines and transformers can be reduced by network reconfiguration, generation rescheduling, and long-term capacity reinforcement. Transient and small-signal stability can be improved by deploying fast-acting protection, FACTS devices, and tuning of Power System Stabilizers (PSSs). Frequency stability remains within the NEA-prescribed  $\pm 2.5\%$  limits; however, increased integration of renewable energy sources in Karnali requires refined planning and operational controls.

## 5. Conclusion

The Karnali province has significant voltage stability challenges due to insufficient generation capacity, high system losses, and overloading of lines and transformers. The Surkhet-Ramghat line and Naumule P/S transformer are overloaded under scenario 2. Most substations in the Karnali province operate below the acceptable lower voltage limit of 0.95 p.u., indicating potential voltage instability.

Based on the PV curve, QV curve, and modal analysis,

the Khalanga S/S is identified as the most voltage instability-prone area. The voltage stability analysis results reveal that the Karnali grid has five potential voltage instability regions (Jumla area, Jajarkot area, Kalikot area, Matela area, and Babiyachaur area). The  $f_{nadir}$  and  $f_{max}$  for the Karnali province power grid are 49.99 Hz and 50.05 Hz (under the largest generator and load outage), respectively, which are within the prescribed limits ( $\pm 2.5\%$ ) by the Nepal Electric Authority. The frequency stability analysis results unveil that the Karnali province power grid is robust to the frequency instability issues. The system's critical clearing time under a symmetrical fault near the largest generator is approximately 0.34 seconds in scenario 3. Small signal stability analysis shows Karnali province power grid has one critical mode, with the local mode poorly damped ( $\approx 5.6\%$ ) in scenario 2.

## Acknowledgment

This study was funded by the Center for Electric Power Engineering (CEPE), School of Engineering, Kathmandu University, Nepal.

## References

- Cho, Y.-B., Cho, Y.-S., Lee, J.-G., & Oh, S.-C. (2021). Design and implementation of probabilistic transient stability approach to assess the high penetration of renewable energy in Korea. *Sustainability*, 13(8), 4205.
- Eftekharijad, S., Vittal, V., Heydt, G. T., Keel, B., & Loehr, J. (2013). Small signal stability assessment of power systems with increased penetration of photovoltaic generation: A case study. *IEEE transactions on sustainable energy*, 4(4), 960–967.
- Gurung, S., Jurado, F., Naetiladdanon, S., & Sangswang, A. (2020). Comparative analysis of probabilistic and deterministic approach to tune the power system stabilizers using the directional bat algorithm to improve system small-signal stability. *Electric Power Systems Research*, 181, 106176.
- Hatziargyriou, N., Milanovic, J., Rahmann, C., Ajarapu, V., Canizares, C., Erlich, I., Hill, D., Hiskens, I., Kamwa, I., Pal, B., et al. (2020). Definition and classification of power system stability—revisited & extended. *IEEE Transactions on Power Systems*, 36(4), 3271–3281.
- Islam, M. R., Numan, M., Shahzad, M., Islam, M. M., & Rana, M. M. (2017). Voltage and transient stability analysis in Bangladesh's power system network (bpsn). *2017 12th IEEE Conference on Industrial Electronics and Applications (ICIEA)*, 866–870.

- Kundur, P. S., Balu, N. J., & Lauby, M. G. (2017). Power system dynamics and stability. *Power system stability and control*, 3, 700–701.
- Morison, G., Gao, B., & Kundur, P. (1993). Voltage stability analysis using static and dynamic approaches. *IEEE transactions on Power Systems*, 8(3), 1159–1171.
- O’Sullivan, J., Rogers, A., Flynn, D., Smith, P., Mullane, A., & O’Malley, M. (2014). Studying the maximum instantaneous non-synchronous generation in an island system—frequency stability challenges in ireland. *IEEE Transactions on Power Systems*, 29(6), 2943–2951.
- Shi, L., Dai, S., Ni, Y., Yao, L., & Bazargan, M. (2009). Transient stability of power systems with high penetration of dfig based wind farms. *2009 IEEE Power & Energy Society General Meeting*, 1–6.
- Shrestha, R., Parajuli, A., Basukala, M., & Gurung, S. (2024). Identification of critical issues in angle, voltage, and frequency stability of the nepal power system. *IEEE Access*.
- Sun, M., Liu, G., Popov, M., Terzija, V., & Azizi, S. (2021). Underfrequency load shedding using locally estimated rocof of the center of inertia. *IEEE Transactions on Power Systems*, 36(5), 4212–4222.
- Wu, Y.-K., Chang, S. M., & Hu, Y.-L. (2017). Literature review of power system blackouts. *Energy Procedia*, 141, 428–431.

This work is licensed under a [Creative Commons](https://creativecommons.org/licenses/by-nc-nd/4.0/) “Attribution-NonCommercial-NoDerivatives 4.0 International” license.

